

LETTER

Microstructure of interstratified illite/smectite at 123 K: A new method for HRTEM examination

TAKASHI MURAKAMI, TSUTOMU SATO

Department of Environmental Safety Research, Japan Atomic Energy Research Institute, Tokai, Ibaraki 319-11, Japan

TAKASHI WATANABE

Department of Geoscience, Joetsu University of Education, Joetsu, Niigata 943, Japan

ABSTRACT

A method to distinguish unambiguously between smectitic interlayers and illitic interlayers in interstratified illite/smectite (I/S) by high resolution transmission electron microscopy (HRTEM) has been developed. An interstratified I/S specimen was cooled to liquid-N temperature outside the column of an electron microscope and transferred into and kept in the microscope column at 123 K. Smectitic and illitic interlayers are unambiguously differentiated by HRTEM, i.e., smectite remains expanded under a high vacuum. The spacing between two illitic interlayers across a single smectitic interlayer is 2.2–2.5 nm. The smectite content of the I/S specimen determined by TEM is consistent with that by X-ray diffraction analysis. The microstructures described in this sample support the smectite to illite conversion mechanisms, dissolution and precipitation, and layer by layer transformation.

INTRODUCTION

The smectite to illite conversion, resulting from diagenetic and hydrothermal alteration, is an important reaction in low-temperature geological environments. Thus, the mechanisms of this conversion are of wide concern. Although Moore and Reynolds (1989) describe four models for this conversion, no single model can explain all of the observations of the smectite to illite conversion. Transmission electron microscopy (TEM) is now a powerful method for investigation of microstructures at the scale of the smectitic and illitic interlayers (for definitions of the terms smectitic and illitic interlayers, see Güven, 1991); direct observations by TEM, using lattice-fringe imaging, have the great advantage of allowing direct determination of the stacking ordering, smectite to illite ratios, and stacking coherency of interstratified I/S. These observations have provided important information on the microstructures of I/S and the mechanisms of the smectite to illite conversion (Lee et al., 1985; Ahn and Peacor, 1986a; Yau and Peacor, 1987; Ahn and Peacor, 1989; Ahn and Buseck, 1990; Jiang and Peacor, 1990; Środoń et al., 1990; Veblen et al., 1990).

One experimental difficulty with TEM examination of interstratified I/S is the collapse of smectitic interlayers under high vacuum. The collapse gives smectite a layer thickness of 1 nm, the same as that of illite; thus, unambiguous distinction of individual smectitic and illitic

interlayers is not possible. Efforts have been made to distinguish smectite from illite by intercalation of laurylamine (Yoshida, 1973; Lee and Peacor, 1986) and n-alkylamine (Bell, 1986; Vali and Köster, 1986; Vali and Hesse, 1990; Vali et al., 1991) in order to keep smectitic interlayers expanded, but with limited success. Recently the method of Guthrie and Veblen (1989a, 1989b, 1990) based on overfocused images was successfully applied to highly ordered I/S of the type $g \geq 1$ (Ahn and Peacor, 1989; Guthrie and Veblen, 1989a; Veblen et al., 1990); however, the application of this method to I/S of the type $g = 1$ with large proportions of smectite or I/S of the type $g = 0$ has not been shown clearly.

Direct TEM observations of the microstructures of interstratified I/S are important to evaluate which conversion models are consistent with both TEM and X-ray diffraction (XRD) data. The present paper describes a new method to directly observe individual smectitic and illitic interlayers at 123 K.

EXPERIMENTAL

The sample used in the present study is a hydrothermally formed interstratified I/S from Otake, Oita, Japan. The sample was fractionated by centrifugation, and the grains $< 2 \mu\text{m}$ were used for the XRD and HRTEM examinations with and without Mg saturation. The specimen did not contain any X-ray detected impurities, such

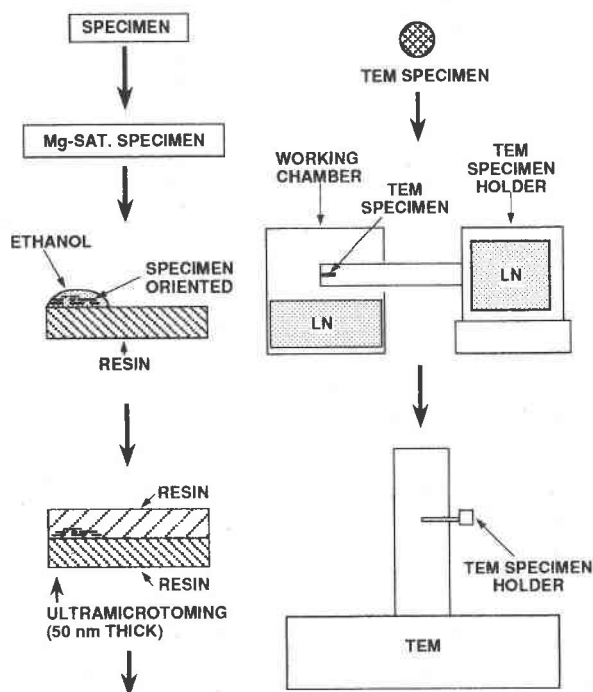


Fig. 1. Schematic of experimental procedure for the TEM examination at 123 K. See text for explanation.

as quartz and mica. The suspension of the Mg-saturated specimen was placed on a glass slide, solvated with ethylene glycol vapor, and then subjected to XRD (a Rigaku powder diffractometer with graphite-monochromatized $\text{CuK}\alpha$ radiation at 40 kV and 20 mA). The comparison of the observed and calculated XRD patterns (Watanabe, 1988) revealed that the specimen was an irregularly interstratified I/S mineral which has Reichweite $g \geq 2$ and 80–85% illite, containing a small amount of I/S with $g = 1$.

For TEM examination, the Mg-saturated specimen was dispersed in deionized H_2O , and a drop of the suspension was placed on a platy solid resin made of Epon 812 (Fig. 1). Thus, the grains were oriented parallel to the surface of the platy resin (Ahn and Peacor, 1985). Before impregnating the specimen in a low-viscosity resin (Epon 812), a drop of ethanol was put on the air-dried, oriented specimen to ensure the impregnation of the resin into the interstices of the specimen grains. After polymerization of the resin, the specimen was cut to be approximately perpendicular to the silicate layers by ultramicrotomy (Reichert-Jung Ultracut E-Microtome), creating sections 50 nm in thickness. The sections were then put on Cu grids with a C substrate and given a conductive C coating by vacuum evaporation. The C-coated TEM specimen was frozen down to liquid-N temperature in a Gatan cryotransfer system. The low temperature and dry atmosphere of the working chamber of the cryotransfer system and the specimen shutter of the TEM holder prevented the specimen from frosting markedly before the

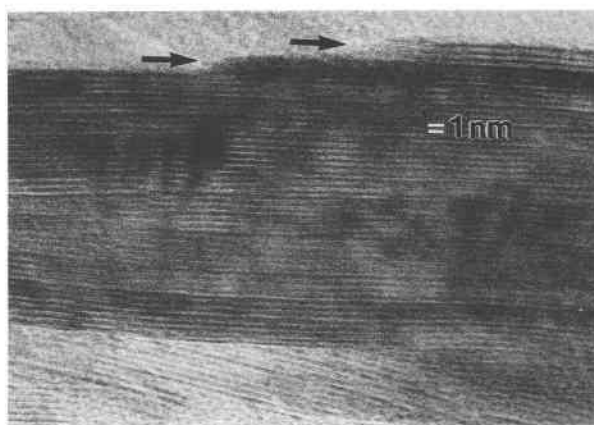


Fig. 2. HRTEM micrographs of the interstratified I/S at room temperature. Focus is near Scherzer. Smectitic interlayers are not distinct from illitic interlayers.

holder was attached to the column of the electron microscope (Fig. 1).

Because the c^* axes of most I/S grains were approximately perpendicular to the electron beam, as mentioned above, lattice fringe images were obtained easily at 200 keV using a Jeol 2000FX microscope. The specimen was kept at 123 K during the TEM examination. The content of expandable (smectitic) interlayers was determined by counting expanded and nonexpanded (illitic) interlayers directly in TEM micrographs. For comparison, a non-frozen I/S specimen of the same material not solvated by Mg was also observed by TEM at room temperature.

Lattice fringe images of the present I/S specimen were interpreted based on the computer simulations by Guthrie and Veblen (1989a, 1989b, 1990); thick dark fringes overlie smectitic interlayers, and thin dark fringes overlie illitic interlayers under appropriate TEM conditions. The charge and Si/Al ratios in the 2:1 layers in the I/S were assumed to be symmetrical across the interlayers, but not symmetrical across the octahedral sheets (e.g., Ahn and Peacor, 1986b). The layer sequences of the lattice fringe images were examined carefully to determine whether there was any inconsistency between the TEM and XRD results.

RESULTS AND DISCUSSION

At low magnification (up to $300\,000\times$ after enlargement), the textures of the I/S at room temperature and 123 K are similar; both consist of packets of layers 5–10 nm thick. The packets of layers are related by low angle boundaries or by a common c^* axis. The length of packet, i.e., the length of the I/S in the ab plane, is several hundred nanometers. The higher content of illite (80–85% by XRD) may result in large domains of I/S (Inoue et al., 1988), which facilitates the TEM observations of the interstratified I/S.

The HRTEM micrograph of the I/S specimen at room temperature is shown in Figure 2. There is no distinction

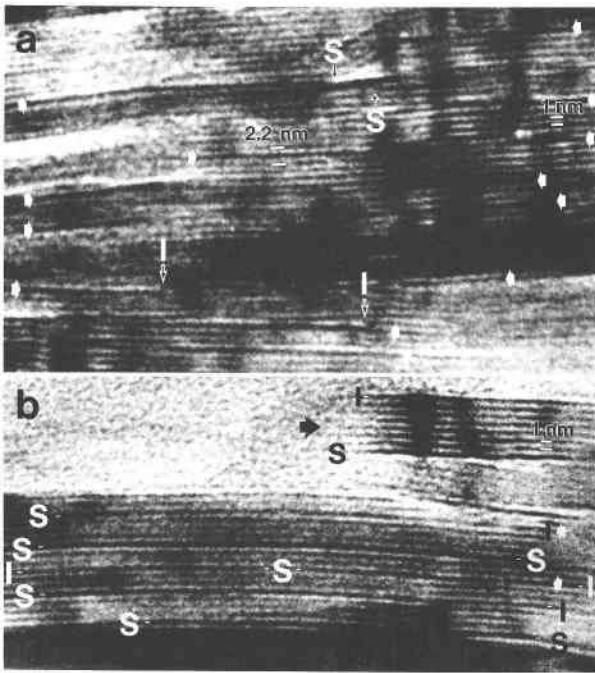


Fig. 3. (a) HRTEM micrograph of the interstratified I/S at 123 K. Defocus is about +150 nm. The white arrows indicate smectitic interlayers. The black arrows with S (smectite) and I (illite) indicate edge dislocations accompanied by smectitic and illitic interlayers, respectively. (b) HRTEM micrograph of the interstratified I/S at 123 K. Defocus is about +150 nm. S denotes part of a smectitic interlayer; I, part of an illitic interlayer. The black arrow indicates a packet bounded by an illitic interlayer at one end and a smectitic interlayer at the opposite end. See text for an explanation of the white arrows.

between smectite and illite; both have 1-nm basal spacing because of the collapse of smectitic interlayers under high vacuum. Packets with a wedged intergrowth structure having steps 3 nm high (arrows in Fig. 2) were observed that may be compared with similar steps (2 nm high) of rectorite (Ahn and Peacor, 1986b).

Smectitic interlayers were unambiguously differentiated (as thicker dark fringes) from illitic interlayers at 123 K (white arrows in Fig. 3a). The spacing between two illitic interlayers across a single smectitic interlayer is 2.2–2.5 nm (Fig. 3a), which corresponds to a combined value of $d(001)$ values for illite and expanded smectite. In over-focused images of ordered I/S with $g = 1$ and with smectitic interlayers collapsed at room temperature, the above spacing was observed up to 2.0 nm, although smectitic interlayers were distinguished by the thicker fringes as compared with those of illitic interlayers (Veblen et al., 1990). However, the simulated image of ordered I/S with $g = 1$ and with smectitic interlayers expanded from 1.0 to 1.2 nm indicating that, by contrast, at a defocus of +50 nm thin dark fringes overlie smectitic interlayers, and thick dark fringes overlie illitic interlayers (Guthrie and Veblen, 1990).

In order to compare the illite content of the I/S speci-

men observed by TEM with that observed by XRD, we directly counted expanded and nonexpanded interlayers (thick and thin dark fringes, respectively) in the TEM micrographs. Eighty-five smectitic interlayers are present in 450 I/S layers, which suggests 81% illite in the I/S specimen. The TEM result (81% illite) is consistent with the XRD result (80–85% illite). Because consistent estimates by XRD and TEM have been previously reported (Środoń et al., 1990), the consistent results of this study confirm that the thick dark fringes distinguished by TEM correspond to smectitic interlayers; the thin dark fringes, to illitic interlayers. Two to ten consecutive interlayers of illite are generally inserted between two smectitic interlayers, which agrees with the XRD results that the specimen is an irregularly interstratified I/S with $g \geq 2$. The sequence SISIS is also found. Thus the layer sequence observed by TEM is completely consistent with that by XRD.

The I/S specimen is characterized by frequently observed edge dislocations, at which smectitic and illitic interlayers are terminated. Figure 3a demonstrates such dislocations by black arrows in S (smectite) and I (illite). Similar layer terminations, which result from the insertion of hydroxide sheets and the removal of tetrahedral sheets, have been observed for the biotite to chlorite conversion (Veblen and Ferry, 1983; Eggleton and Banfield, 1985). If the smectite to illite conversion is due to a dissolution and precipitation mechanism (e.g., Inoue et al., 1987), the smectitic interlayer terminations suggest the dissolution of pairs made up of a smectitic interlayer and a 2:1 layer, and the illite layer terminations suggest the precipitation of pairs made up of an illitic interlayer and a 2:1 layer.

The thickness of a fringe sometimes changes if the fringe is traced along its length (Fig. 3b). A fringe starting as a smectitic interlayer on the left of the micrograph becomes an illitic interlayer on the right (upper white arrow in Fig. 3b) whereas the next smectitic interlayer maintains its thickness. Another fringe starting as an illitic interlayer to the left becomes a smectitic interlayer in the middle and finishes as an illitic interlayer again (lower white arrow in Fig. 3b). This could suggest that part of a smectitic interlayer collapses where the thickness is the same as that of an illitic interlayer. However, the statistics of counting fringes in the TEM micrographs revealed that the smectitic interlayers do not completely collapse, as previously mentioned. Therefore, the change in thickness observed is indeed due to the smectite to illite conversion. The thickness change suggests the layer by layer transformation of smectite to illite without dissolution and precipitation.

With either mechanism, dissolution and precipitation or layer by layer transformation, the areas in which the dislocations and the layer thickness changes occur suggest that the smectite to illite reaction frequently takes place within grains. These reaction areas may be compared with those observed in the biotite chloritization (Veblen and Ferry, 1983; Eggleton and Banfield, 1985).

ACKNOWLEDGMENTS

The authors are grateful to K. Fukai for the use of a transmission electron microscope, Jeol 2000FX. We thank A. Inoue at Chiba University and R.C. Ewing for the critical reviews of an early version of the manuscript. Constructive comments by the reviewers D.R. Veblen and H. Vali are gratefully acknowledged.

REFERENCES CITED

- Ahn, J.H., and Buseck, P.R. (1990) Layer-stacking sequences and structural disorder in mixed-layer illite/smectite: Image simulations and HRTEM imaging. *American Mineralogist*, 75, 267–275.
- Ahn, J.H., and Peacor, D.R. (1985) Transmission electron microscopic study of diagenetic chlorite in Gulf Coast argillaceous sediments. *Clays and Clay Minerals*, 33, 228–236.
- (1986a) Transmission and analytical electron microscopy of the smectite-to-illite transition. *Clays and Clay Minerals*, 34, 165–179.
- (1986b) Transmission electron microscope data for rectorite: Implications for the origin and structure of “fundamental particles.” *Clays and Clay Minerals*, 34, 180–186.
- (1989) Illite/smectite from Gulf Coast shales: A reappraisal of transmission electron microscope images. *Clays and Clay Minerals*, 37, 542–546.
- Bell, T.E. (1986) Microstructure in mixed-layer illite/smectite and its relationship to the reaction of smectite to illite. *Clays and Clay Minerals*, 34, 146–154.
- Eggleton, R.A., and Banfield, J.F. (1985) The alteration of granitic biotite to chlorite. *American Mineralogist*, 70, 902–910.
- Guthrie, G.D., Jr., and Veblen, D.R. (1989a) High-resolution transmission electron microscopy applied to clay minerals. In L.M. Coyne, D.F. Blake, and S. McKeever, Eds., *Spectroscopic characterization of minerals and their surfaces*. American Chemical Society Symposium Series, 415, 75–93.
- (1989b) High-resolution transmission electron microscopy of mixed-layer illite/smectite: Computer simulations. *Clays and Clay Minerals*, 37, 1–11.
- (1990) Interpreting one-dimensional high-resolution transmission electron micrographs of sheet silicates by computer simulation. *American Mineralogist*, 75, 276–288.
- Güven, N. (1991) On a definition of illite/smectite mixed-layer. *Clays and Clay Minerals*, 39, 661–662.
- Inoue, A., Kohyama, N., Kitagawa, R., and Watanabe, T. (1987) Chemical and morphological evidence for the conversion of smectite to illite. *Clays and Clay Minerals*, 35, 111–120.
- Inoue, A., Velde, B., Meunier, A., and Touchard, G. (1988) Mechanism of illite formation during smectite-to-illite conversion in a hydrothermal system. *American Mineralogist*, 73, 1325–1334.
- Jiang, W.T., and Peacor, D.R. (1990) Transmission and analytical electron microscopic study of mixed-layer illite/smectite formed as an apparent replacement product of diagenetic illite. *Clays and Clay Minerals*, 38, 449–468.
- Lee, J.H., and Peacor, D.R. (1986) Expansion of smectite by laurylamine hydrochloride: Ambiguities in transmission electron microscope observations. *Clays and Clay Minerals*, 34, 69–73.
- Lee, J.H., Ahn, J.H., and Peacor, D.R. (1985) Textures in layered silicates: Progressive changes through diagenesis and low-temperature metamorphism. *Journal of Sedimentary Petrology*, 55, 532–540.
- Moore, D.M., and Reynolds, R.C., Jr. (1989) X-ray diffraction and the identification and analysis of clay minerals, p. 332. Oxford University Press, New York.
- Šrodoň, J., Andreoli, C., Elsass, F., and Robert, M. (1990) Direct high-resolution transmission electron microscopic measurement of expandability of mixed-layer illite/smectite in bentonite rock. *Clays and Clay Minerals*, 38, 373–379.
- Vali, H., and Hesse, R. (1990) Alkylammonium ion treatment of clay minerals in ultra thin section: A new method for HRTEM examination of expandable layers. *American Mineralogist*, 75, 1443–1446.
- Vali, H., and Köster, H.M. (1986) Expanding behaviour, structural disorder, regular and random irregular interstratification of 2:1 layer-silicates studied by high-resolution images of transmission electron microscopy. *Clays and Clay Minerals*, 24, 827–859.
- Vali, H., Hesse, R., and Kohler, E.E. (1991) Combined freeze-etch replicas and HRTEM images as tools to study fundamental particles and the multiphase nature of 2:1 layer silicates. *American Mineralogist*, 76, 1973–1984.
- Veblen, D.R., and Ferry, J.M. (1983) A TEM study of the biotite-chlorite reaction and comparison with petrologic observations. *American Mineralogist*, 68, 1160–1168.
- Veblen, D.R., Guthrie, G.D., Jr., Livi, K.J.T., and Reynolds, R.C., Jr. (1990) High-resolution transmission electron microscopy and electron diffraction of mixed-layer illite/smectite: Experimental results. *Clays and Clay Minerals*, 38, 1–13.
- Watanabe, T. (1988) The structural model of illite/smectite interstratified mineral and the diagram for its identification. *Clay Science (Japan)*, 7, 97–114.
- Yau, Y.-C., and Peacor, D.R. (1987) Smectite-to-illite reactions in Salton Sea shales: A transmission and analytical electron microscopy study. *Sedimentary Petrology*, 57, 335–342.
- Yoshida, T. (1973) Elementary layers in the interstratified clay minerals as revealed by electron microscopy. *Clays and Clay Minerals*, 21, 413–420.

MANUSCRIPT RECEIVED NOVEMBER 12, 1992

MANUSCRIPT ACCEPTED FEBRUARY 11, 1993